Proc. Natl. Acad. Sci. USA
Vol. 94, pp. 6694–6699, June 1997
Biochemistry

Monomeric isomers of human interleukin 5 show that 1:1 receptor recruitment is sufficient for function

JUN LI*†, RICHARD COOK*, MICHAEL L. DOYLE‡, PRESTON HENSLEY‡, DEAN E. MCNULTY§, AND IRWIN CHAIKEN¶‖

Departments of *Molecular Immunology, ‡Macromolecular Sciences, and §Protein Biochemistry, SmithKline Beecham Pharmaceuticals, 709 Swedeland Road, King of Prussia, PA 19406; and ¶Rheumatology Division, Department of Medicine, University of Pennsylvania School of Medicine, 913 Stellar Chance Laboratories, 422 Curie Boulevard, Philadelphia, PA 19004

Communicated by David S. Eisenberg, University of California, Los Angeles, CA, April 16, 1997 (received for review February 11, 1997)

ABSTRACT **The normally dimeric human interleukin 5 (IL-5) was re-engineered into two monomeric isomer forms to investigate mechanistic features of receptor recognition. One form, denoted GM1–IL-5, is a CD-loop expanded form, in which an 8-residue linker designed for flexibility was inserted between residues 85 and 86. The second, denoted DABC–IL-5, is a circularly permuted form of human IL-5 in which a chain discontinuity was introduced in the CD loop and the two consequent chain fragments were joined at the normal N and C termini by a di-glycyl linker. Both IL-5 isomers folded into stable monomers in solution as shown by sedimentation equilibrium and CD and formed an intrachain disulfide bond predicted from the structure of wild type IL-5. From titration microcalorimetry and optical biosensor analyses, both monomers were shown to interact with the IL-5 receptor α chain with 1:1 stoichiometry and affinities 30- to 40-fold weaker than for the dimeric wild type protein. And both monomers stimulated cell proliferation of human IL-5 receptor positive cells with a concentration dependence close to that of wild type. The data show that both monomeric and dimeric forms of IL-5 function through similar 1:1 receptor α chain recruitment processes and that it is the helical packing of the monomeric four-helix bundle unit in IL-5, rather than the helical connectivity itself, that appears to play the major role in presenting structural epitopes to trigger functional receptor activation.**

Human interleukin 5 (hIL-5) is a hematopoietic growth factor protein implicated in the development of eosinophil-dependent allergic reactions (1, 2). The high-resolution structure of hIL-5 determined crystallographically shows a dimeric core of two four-helix bundles formed by two identical polypeptide chains joined covalently by disulfide bonds (3, 4). The two-bundle structure of the IL-5 dimer is formed by helix swapping (5), in which the helix D from one chain combines with helices A, B, and C from the second chain to form each of the two four-helix bundle domains. Nonetheless, each 4-helix bundle resembles the four-helix bundle of two monomeric cytokines, IL-3 (6) and granulocyte-macrophage colony-stimulating factor (GM-CSF) (7), which together with IL-5 comprise a family of short chain hematopoietic cytokines with eosinophil differentiation and activation properties. Furthermore, IL-3, IL-5, and GM-CSF all share a similar two-subunit receptor composition, in each case composed of an α chain specificity subunit, which provides most of the binding energy for cytokine recognition, and an identical β_c chain subunit, which is required for signal transduction and consequent cell regulation and growth (8, 9). In spite of its unique dimer character, IL-5 shows a 1:1 stoichiometry for IL-5 receptor α chain (IL-5Rα) binding (4, 10), similarly as would be expected for the monomeric IL-3 and GM-CSF with their respective α subunits. This leads to the question of why IL-5 is a dimer and whether being dimeric has structural and functional consequences.

These questions have led to the effort to reconstruct IL-5 into monomeric forms and to determine their functional and structural properties. Based on the superposition of the high-resolution structures of GM-CSF and IL-5, it was proposed that the IL-5 dimer might have been a monomer, and a loop deletion between helix C and D forced it instead to adopt an open D-helix swapped dimeric structure (5). This inferred that lengthening the CD loop could allow the IL-5 chain to fold into a monomer. Indeed, Dickason and Huston (11) described a biologically active IL-5 monomer (mono 5) in which the length of the CD loop of hIL-5 was increased to that of monomeric GM-CSF. The results with mono 5 showed that the single four-helix bundle domain of IL-5 contains sufficient structure to induce biological function. However, mono 5 had about a 1 order of magnitude higher EC_{50} and 2 orders of magnitude lower receptor α chain affinity than wild-type IL-5 (wtIL-5) (12). The introduction of the eight residues from the CD loop of GM-CSF appeared to have destabilized the conformation of IL-5, as judged by lack of formation of the disulfide bond, between the two cysteine residues in the CD loop, which was expected if the monomer folded as predicted for a single four-helix bundle. Furthermore, receptor stoichiometry was not determined for this original mono 5 construction. Nonetheless, its discovery demonstrated the feasibility to make active IL-5 monomers.

We were interested to use monomeric forms of IL-5 to investigate mechanistic features of receptor recognition and activation and hence sought to obtain monomeric constructions with strong stability, receptor affinity, and bioactivity. To do this, we also focused on CD loop enlargement as originally suggested by Bennett *et al.* (5). In addition, we also considered circular permutation. Circularly permuted proteins are generated by connecting their normal termini covalently and introducing breaks at other sites to produce new termini (13, 14). Proteins whose N and C termini are flexible and in close proximity are candidates for circular permutation, as exemplified previously with aspartate transcarbomylase (15), mu-

Abbreviations: GM-CSF, granulocyte-macrophage colony-stimulating factor; hIL-5, human interleukin 5; DABC–IL-5 (or DABC for short), the protein engineered derivative of IL-5 in which the order of helical segments from the amino to carboxyl terimus is D to A to B to C; GM1–IL-5 (or GM1 for short), protein-engineered derivative of IL-5 in which the CD loop of IL-5 has an eight-residue insertion between residues 85 and 86; mono 5, monomeric IL-5; scIL-5, single chain IL-5; IL-5Rα, IL-5 receptor α chain; MALDI-MS, matrix-assisted laser desorption ionization mass spectrometry; RU, response units; shIL-5Rα, soluble hIL-5 receptor α chain; wt, wild type; β_c, β chain of IL-5 receptor which is also common to the receptors of IL-3 and GM-CSF.

†Present address: Department of Immunological Diseases, Boehringer Ingelheim Pharmaceuticals, 900 Ridgebury Road, Ridgefield, CT 06877.
‖To whom reprint requests should be addressed.

The publication costs of this article were defrayed in part by page charge payment. This article must therefore be hereby marked "*advertisement*" in accordance with 18 U.S.C. §1734 solely to indicate this fact.

rine dihydrofolate reductase (16), T4 lysozyme (17), and human IL-4 (18).

In this paper, we report the design and expression of two monomeric forms of IL-5. One, denoted GM1–IL-5 (or GM1), is a CD-loop expanded form, while the second, denoted DABC–IL-5 (or DABC), is a circularly permuted form of wtIL-5. We demonstrate that both IL-5 isomers fold into stable monomers in solution. The receptor affinity and α subunit stoichiometry properties argue that both monomeric and dimeric forms of IL-5 function through similar 1:1 receptor subunit recruitment processes. This work establishes the GM1 and DABC monomers as viable tools for mutagenesis, phage display, and evaluating common features in receptor activation and signal triggering in IL-5 and its hematopoietic cytokine family.

METHODS

Construction of DABC and GM1 Genes. pCDN–scIL-5 encodes a single chain form of dimeric IL-5 that contains two IL-5 chains connected with a flexible Gly-Gly linker (19). It was used as a template for the PCR to generate DABC gene fragment. The 5′ primer used in this PCR encodes residues 86–115 of IL-5, and the 3′ primer encodes residues 75–84 of IL-5. The amplified DNA fragment (≈350 bp) was digested with *Bam*HI and inserted into the *Bam*HI site of Baculovirus expression vector pFastBacI (GIBCO/BRL), yielding pFastBacI–DABC. The protein sequence for the expressed DABC is GARS-[IL-5_{86-115}–*GG*RS-IL-5_{4-85}]. The GARS sequence was from the tissue plasminogen activator leader sequence used in expression.

pCDN–IL-5 (20) was used as a PCR template for generating DNA fragments containing wtIL-5 or GM1–IL-5. The PCR products were ligated into the *Bam*HI site of pFastBacI, yielding pFastBacI–wtIL-5 and pFastBacI–GM1. The protein sequence for wtIL-5 is GARS-IL-5_{4-115}. The protein sequence for GM1 is GARS-IL-5_{4-85} *GGSGGSGG*-IL-5_{86-115}. The peptide linker *GGSGGSGG* in GM1 was introduced by two overlapping PCR primers.

Protein Expression and Purification. pFastBacI plasmid DNAs harboring wtIL-5, GM1, or DABC were transfected into Sf21 cells and the latter grown in serum-free medium following standard protocols (21). wtIL-5 and monomeric IL-5 isomers were secreted into the medium. Cell media were harvested 72 h after transfection and purified chromatographically using agarose-immobilized anti-IL-5. The column was washed with PBS and eluted with a solution containing 0.1 M glycine (pH 2.2), 2 mM EDTA, and 1 mM phenylmethylsulfonyl fluoride. The eluted fractions were neutralized immediately with 1 M Tris (pH 9.0). Pooled protein solutions were concentrated and changed into PBS buffer by ultrafiltration (Amicon). Protein concentrations were determined by amino acid analysis.

Equilibrium Sedimentation. Analytical ultracentrifuge data were collected in a Beckman XL-I analytical ultracentrifuge using double sector cells with sapphire windows (22). The primary data, absorbance at 280 nm versus radius, were fit as described in Chan *et al.* (23). The partial specific volume was estimated to be 0.741 ml/g for IL-5 DABC and GM1 (4), and the solvent density was estimated to be 1.006 ml/g (24). The solvent was 150 mM NaCl and 10 mM phosphate (pH 7.4). The molecular mass of the monomer was determined by matrix-assisted laser desorption ionization mass spectrometry (MALDI-MS) to be 14,352 Da (for DABC; data not shown). The test for equilibrium was the superposition of curves taken 4 h apart.

Kinetics Analysis of Receptor Binding. Kinetic and equilibrium constants for the interaction between hIL-5Rα and different forms of hIL-5 were measured using a BIAcore 1000 optical biosensor in a sandwich capture assay similar to that described previously (19, 20, 25). A rat anti-IL-5 mAb 4A6, which does not neutralize the IL-5Rα interaction, was immobilized onto the biosensor CM5 chip. The purified wtIL-5 and monomeric IL-5 isomers were anchored noncovalently, but tightly, to mAb 4A6 and the binding of various concentrations of soluble hIL-5Rα (shIL-5Rα) to the attached IL-5 was then measured.

For data analysis of sensorgrams obtained for a series of shIL-5Rα concentrations (26), the linear portion of the association phase and first 25 sec of dissociation phase were used to calculate k_{on} and k_{off}, respectively. K_d was determined from the ratio k_{off}/k_{on}. In addition, the maximum response unit (RU) values (R_{max}) of the association phases, taken as the steady-state amount bound at different receptor concentrations, were used to determine a steady-state derived K_d and stoichiometry n from nonlinear least squares fit of R_{max} vs. [shIL-5Rα].

Cell Proliferation Activity. Biological activity was determined by cell proliferation using both human-derived TF-1.28 cells (19) and murine-derived B13 cells (4).

Isothermal Titration Calorimetry. Titration calorimetry experiments were carried out with a Microcal (Amherst, MA) MCS isothermal titration calorimeter. Protein concentrations were measured by absorbance at 280 nm. Molar extinction coefficients, calculated from amino acid sequence using the relationship reported by Pace *et al.* (27), were 17,000, 8,800, 8,700, and 68,000 for wtIL-5 (dimer), DABC (monomer), GM1 (monomer), and IL-5Rα, respectively. Calorimetry data were analyzed with Microcal ORIGIN software according to a single-site binding model in each case (28). The model includes an equilibrium binding constant, a molar binding enthalpy change, and a molar binding ratio.

Circular Dichroism. CD measurements were made on a Jasco (Easton, MD) J-710 spectropolarimeter in a 0.1 cm water-jacketed cuvette. Solution conditions were 0.2 mg/ml protein (pH 7.4), 20 mM sodium phosphate, and 150 mM NaCl at 25°C. Spectra shown are the average of three scans run at 50 nm per minute with a 2-sec response time. Thermal stabilities of IL-5 constructs were evaluated by monitoring the ellipticity at 222 nm. Temperature was increased in each case at a rate of 50°C per hour.

Mass Spectrometry. MALDI-MS data were obtained with a PerSeptive Biosystems Voyager RP laser desorption time-of-flight mass spectrometer (PerSeptive Biosystems, Framingham, MA). Samples were diluted 1:5 with 3,5-dimethoxy-4-hydroxy-cinnamic acid (10 mg/ml in 2:1 0.1% trifluoroacetic

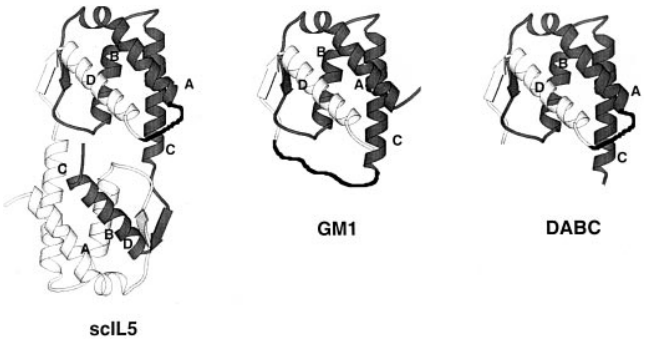

FIG. 1. Schematic structural diagram of scIL-5, DABC, and GM1. (*Left*) scIL-5. The two hIL-5 polypeptide chains are denoted in dark and light shades of grey. The two chains are connected by a dark ribbon (hand drawn) representing the Gly-Gly linker connecting the C terminus of one chain and the N terminus of the another chain. The helices A, B, C, and D of chain a are denoted. Structure derived from Milburn *et al.* (3). (*Center*) GM1. The dark ribbon designates the *GGSGGSGG* linker inserted between residue 85 and 86. (*Right*) DABC. This consists of the upper domain of scIL-5. The truncations are made between residue 85 and 86 of IL-5.

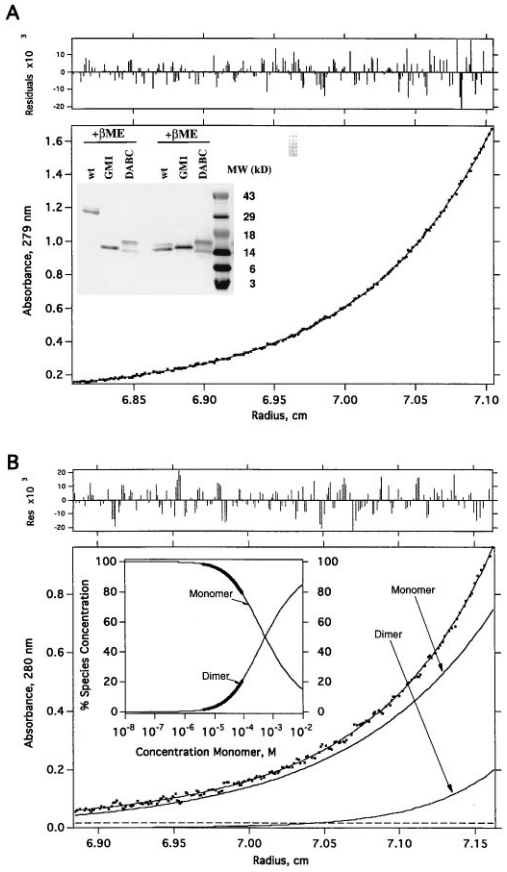

FIG. 2. Size analyses of DABC and GM-1. (*A*) Equilibrium sedimentation data of DABC in 150 mM NaCl and 20 mM phosphate (pH 7.4). Initial loading concentrations were $\approx 0.3 A_{280}$ ($\approx 32\ \mu$M). The protein was centrifuged for >20 h at 20°C, until equilibrium was reached (see *Methods*). The molecular mass determined from this analysis was 14,966 ± 49 Da. There was no evidence of self-assembly to the dimeric form. (*Upper*) The distribution of residuals for the fit of the primary data (absorbance at 280 nm vs. radius) to a model for a single species (23) is shown. (*Inset*) SDS/PAGE analysis. Affinity purified samples ($\approx 2\ \mu$g) were run on a 16% gel either reducing (*Right*) or nonreducing (*Left*). (*B*) Equilibrium sedimentation data for GM1. The data were fit with $K_{1,2} = 5.2 \pm 0.4 \times 10^{-4}$ M. Shown also are the individual curves computed, according to the analysis, for monomer and dimer separately. Experimental conditions are the same as for the DABC data (*A*). (*Upper*) The distribution of residuals for the fit of the primary data, a monomer-dimer equilibrium (23) is shown. (*Inset*) This shows the fraction of monomer and dimer as a function of total protein concentration computed from an analysis of the data according to a monomer-dimer model. The bold portions of the curves indicate the concentration ranges over which the data were actually fit. The thin portions of the curves are extrapolations according to the model. From this analysis one can show that at a total GM1 concentration of 10^{-5} M, the fraction of dimer is 3.5%.

acid/acetonitrile) for a final protein concentration of 1–10 pmol/μl. Bovine β lactoglobulin A (Sigma) was included as an internal calibrant (MH+, 18,364 Da). Desorption/ionization was accomplished using photon irradiation from a 337-nm pulsed nitrogen laser and 25-keV accelerating energy. Spectra were averaged over ≈100 laser scans.

RESULTS

Construction and Expression of IL-5 Monomers. Design of the permuted monomeric IL-5, DABC, was based on the previous construction of scIL-5 (19). As shown in Fig. 1, the scIL-5 molecule (Fig. 1 *Left*) was cut into two domains by making truncations at the two CD loop regions, thus transforming the upper domain of scIL-5 into a permuted mono 5 (Fig. 1 *Right*). The dipeptide -Gly-Gly was used to link the C terminus (after helix D) and the N terminus (before helix A). Since scIL-5 contains the same Gly-Gly linker and exhibits the same receptor binding affinity and biological activity as those of wtIL-5, the linker was not expected to distort the conformation of the DABC molecule significantly.

Design of the nonpermuted IL-5 monomer, denoted GM1, was based on sequence alignment and structure comparison between IL-5 and GM-CSF (5). In that work, it was predicted that extending the length of CD loop of IL-5 might result in a monomer containing one four-helix bundle. A flexible peptide linker Gly-Gly-Ser-Gly-Gly-Ser-Gly-Gly- was inserted between residue Lys-85 and Cys-86 of human IL-5. The structure of GM1 is shown in Fig. 1 *Center*.

DABC and GM1 showed similar molecular weights (14–16 kDa) to that of wtIL-5 under reducing conditions (Fig. 2). Under nonreducing conditions, DABC and GM1 still ran as monomers (14–16 kDa), while wtIL-5 migrated as a dimer (≈28 kDa). The two bands of DABC (14 kDa and 16 kDa) both have the complete predicted protein sequence, based on N-terminal sequencing and amino acid analysis (data not shown). The difference in molecular weight is probably due to different glycosylation levels. The fact that DABC and GM1 have the same molecular weights under nonreducing conditions indicated that no intermolecular disulfide bonds had formed in the two IL-5 monomers.

Folding Properties of DABC and GM1. DABC and GM1 were both shown to form monomers by sedimentation equilibrium analysis. As shown in Fig. 2, DABC has no significant tendency to dimerize and is monomeric throughout the concentration gradient of the centrifuge run. In contrast, GM1 aggregates to dimer at concentrations above 10 μM.

To directly compare the secondary structures and their stabilities, CD was measured for wtIL-5, DABC, and GM1. As shown in Fig. 3, the similarity of spectra for the three IL-5 forms indicates that the monomeric constructs likely are folded into similar secondary structures as wtIL-5. The shapes of the spectra are consistent with large α helical contents. Thermal stabilities of IL-5 constructs were evaluated by CD (Fig. 3). The monomers were found to have considerably reduced stability compared with dimeric wtIL-5. Although their half-

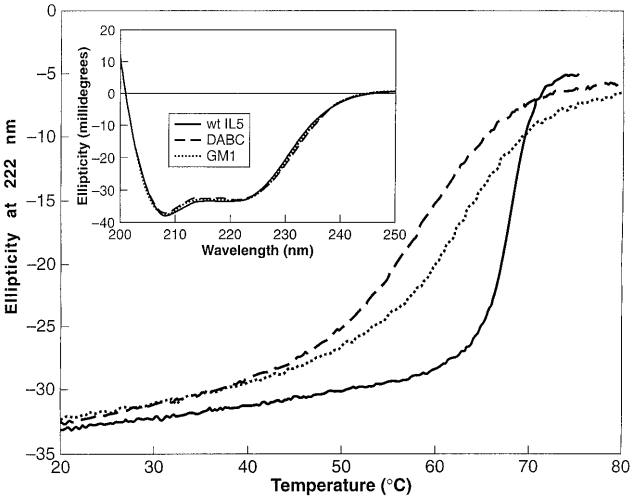

FIG. 3. CD of wtIL-5, DABC, and GM1. Thermal stability of IL-5 constructs was evaluated with a Jasco J-710 spectropolarimeter by monitoring the ellipticity at 222 nm in a 0.1 cm water-jacketed cuvette. Solid line, wtIL-5; dashed line, DABC; dotted line, GM1. (*Inset*) CD spectra at 25°C for the three forms of IL-5 as denoted in main figure. Conditions were the same as in the thermal stability measurements. Spectra shown are the average of three scans run at 50 nm per minute with a 2-sec response time.

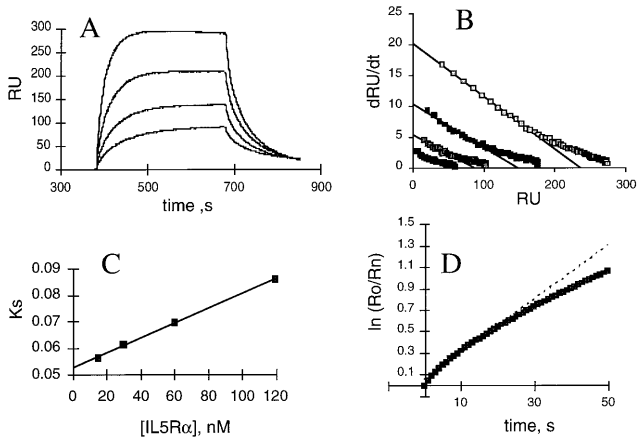

FIG. 4. Binding kinetics of DABC with shIL-5Rα. (*A*) Overlays of sensorgrams for binding of various concentrations of shIL-5Rα to DABC captured by mAb 4A6 on the sensor chip. Receptor samples of 15, 30, 50, and 120 nM were injected. The increase in response shows the binding of shIL-5Rα. The flattened plateau indicates equilibrium is reached. The decay represents the dissociation of bound shIL-5Rα. Data analyses in *B–D* were as described (26). (*B*) *dR/dt* plots of association data. The slopes of the linear portions of these plots yield k_s values. (*C*) k_s plot. The slope of this plot yields k_{on}. (*D*) Natural log plot of dissociation data for 120 nm shIL-5Rα sensorgram. The linear fit of the first 25 sec of data yielded k_{off}.

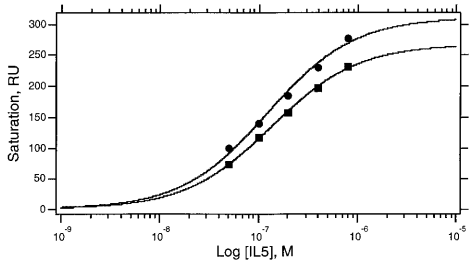

FIG. 5. Stoichiometry analysis of DABC–shIL-5Rα (●) and GM1–shIL-5Rα (■) complexes. Variations of binding response at steady state (plateau in association phase, see Fig. 4*A*) with receptor concentration were fitted by nonlinear least squares methods to a single site binding model (rectangular hyperbola) to determine the stoichiometry (molecules of receptor bound per molecule of IL-5 isomer) and steady-state K_d values given in Table 1.

unfolded T_m values were only 4–8 degrees lower than wtIL-5, the monomers exhibited much broader unfolding curves and began to unfold near physiological temperature. Analysis of the unfolding curves assuming a two-state model** (29) predicts that wtIL-5 is 65,000-fold more stable than DABC at 37°C. It may be that part of the biological role for the dimeric form is to stabilize IL-5 against thermally induced degradation pathways and/or proteolysis.

Cys-44 and Cys-86 form two interchain disulfide bonds in wtIL-5. In the structures of DABC and GM1 predicted from the wtIL-5 structure, these two cysteine residues would be proximate to each other and hence might be expected to form an intrachain disulfide bond. To test whether this disulfide bond is preserved in the mono 5 forms made here, DABC and GM1 (10 μM in PBS) were reacted with 10 mM iodoacetamide (Fluka) for 1 h at 25°C in the dark. In both cases, the proteins showed no mass shift by MALDI-MS. However, when DABC and GM1 were preincubated with 5 mM dithiothreitol (Calbiochem) at 50°C for 30 min prior to iodoacetamide treatment, MALDI-MS showed the predicted 114-Da mass shift consistent with carboxamidomethylation of the two cysteine residues. These results confirmed the presence of the intramolecular disulfide bond in both DABC and GM1, suggesting that the tertiary structures of DABC and GM1 are very close to those expected for a single four-helix bundle half of the wtIL-5 structure.

Finally, both GM1 and DABC were shown by optical biosensor analysis to bind tightly to two conformationally dependent IL-5 mAbs (4A6 and 2B6) (data not shown), indicating that DABC and GM1 fold into similar four-helix bundle structures as that of wtIL-5. Indeed, the extremely slow dissociation ($k_{off} < 10^{-4}$·s^{-1}) of the 4A6 complexes allowed capture of monomeric IL-5 isomers on the biosensor chip for analysis of IL-5Rα binding kinetics (see below).

Affinities of DABC and GM1 for IL-5Rα. Kinetics of shIL-5Rα binding to antibody-anchored monomers were measured with an optical biosensor. Fig. 4 shows the sensorgrams for DABC and the linear transformations of the association and dissociation phases. Similar data were obtained for GM1 and wtIL-5. As summarized in Table 1, the rate constant-derived K_d values of DABC and GM1 were 100 nM and 105 nM, respectively, as compared with the 2.4 nM affinity of the similarly expressed wtIL-5. There was ≈4 fold difference in k_{on} and 10-fold difference in k_{off} between DABC and wtIL-5. The faster k_{on} for wtIL-5 is expected since the protein has two potential binding modes due to its dimeric nature. The ≈10-fold increase in k_{off} for DABC and GM1 is consistent with the hypothesis that the IL-5–IL-5Rα complex is stabilized by residues from both domains of wtIL-5 molecule (25) and that monomers may have incrementally less contacts than dimers for α subunits. The kinetically derived K_d values were in good agreement with those obtained from steady-state biosensor data and by titration microcalorimetry (see below).

Biological Activities of DABC and GM1. The ability of DABC and GM1 to induce signal transduction was measured by cell proliferation. The maximum bioactivity of DABC and GM1 with TF-1.28 cells was similar to that of wtIL-5 (≈100 pM). The EC_{50} values for DABC and GM1 were 4- and 8-fold greater, respectively, than the EC_{50} value for wtIL-5 (Table 1). The difference is likely due to their lower affinities to the receptor. Biological activity of all three proteins could be completely neutralized by the anti-IL-5 mAbs 2B6 (30) and

**The ability of the two-state model to describe the unfolding curves in Fig. 3 to within instrumental error suggests that these molecules may unfold as single cooperative units. However, it needs to be cautioned that the CD data alone are insufficient to prove rigorously the two-state mechanism.

Table 1. Receptor binding, bioactivity, and stability properties of wtIL5 and monomeric IL-5s

	k_{on}, M^{-1}·$s^{-1} \times 10^{-5}$	k_{off} ($s^{-1} \times 10^{-3}$)	K_d, nM (ratio of rates)	K_d, nM (steady-state)	Stoichiometry, mol shIL5Rα/mol IL5 (from steady-state)	TF-1 EC_{50}, pM	B13 EC_{50}, pM	T_m, °C	ΔH, kcal/mol
wtIL5	10.5 ± 1.3	2.5 ± 0.1	2.4 ± 0.2		0.9 ± 0.1*	3	9	67.9 ± 0.2	155 ± 3
DABC	2.5 ± 0.3	25 ± 0	100 ± 14	134 ± 8	1.1 ± 0.02	12	2,201	59.7 ± 0.5	43 ± 3
GM1	2.2 ± 0.1	23 ± 1	105 ± 4	122 ± 17	1.0 ± 0.08	24	170	63.8 ± 0.2	49 ± 1

Rate constants, equilibrium constants, and stoichiometries were from optical biosensor analyses. TF-1 and B13 cell proliferation activities are given as the concentrations required from half maximal stimulation. Unfolding T_m and ΔH values are from CD measurements.
*For wtIL5, stoichiometry was obtained from extrapolation of kinetic data, and no steady-state K_d is reported, since the kinetic sensorgrams did not form definitive steady state plateaus for this form.

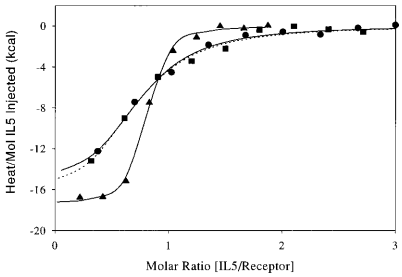

FIG. 6. Titration calorimetry data for dimeric and monomeric forms of IL-5 binding to IL-5R. Heat per mol of IL-5 added at each injection is shown versus the cumulative ratio of IL-5 mol added per mol of receptor. For all cases the ≈75 μM IL-5 construct was titrated as 5–10 μl volumes into the calorimeter which contained 1.3 μM receptor. ▲, wtIL-5; ●, DABC; and ■, GM1. Best-fit regression curves are: wtIL-5 and DABC (solid line), and GM1 (dotted lined). Conditions are as in Table 2.

4A6 (data not shown), indicating the specificity of biological effect.

Interestingly, compared with the response obtained with wtIL-5, DABC and to a lesser extent GM1 showed much lower bioactivity in the B13 cell line than they did in the TF1 cell line. This suggests a loss of conformational binding epitopes in the monomers that are important for recognition and signal triggering of murine but not human receptor.

Stoichiometry of IL-5 Monomer–IL-5Rα Interaction. Dimeric IL-5 has been demonstrated to interact with IL-5Rα with a 1:1 stoichiometry (4, 10). One explanation for this is that the binding surface on IL-5Rα overlaps both four-helix bundle domains. Thus, it was important to determine whether IL-5Rα could associate with two mono 5 molecules and, if so, with what affinity. We used data from the optical biosensor to evaluate the binding stoichiometry of IL-5 monomers. Because the biosensor detector RU is proportional to the protein mass present in the detection volume, the mass ratio of IL-5 and IL-5Rα in a complex can be calculated from their respective contributions. For DABC–IL-5Rα and GM1–IL-5Rα, the response of IL-5Rα at steady-state was read directly from sensorgrams and both K_d and stoichiometry (n) obtained by nonlinear least squares fits of steady-state R_{max} values of shIL-5Rα bound at various concentrations (Fig. 5). As shown in Table 1, DABC and GM1 both bind to IL-5Rα at ≈1:1 stoichiometry. A stoichiometry for wtIL-5 also was estimated from biosensor data, in this case by comparing the extrapolated R_{max} for receptor bound from linearized dR/dt vs. R plots (26) to the RU of wtIL-5 captured on the sensor surface. This method was used since the kinetic sensorgrams did not form definitive steady-state plateaus for wtIL-5. Nonetheless, the 1:1 stoichiometry so measured (Table 1) is similar to that reported before for wtIL-5 (4). The results demonstrate that one four-helix bundle of IL-5 is sufficient to bind one receptor α chain. One limitation of this experiment is that having disperse IL-5 constructs on the sensor surface prejudices against a 2:1 IL-5 monomer: IL-5Rα stoichiometry.

We obtained additional evidence for 1:1 stoichiometry using titration microcalorimetry. Fig. 6 shows calorimetry data for the titration of IL-5R with each of wtIL-5, DABC, and GM1. The affinity, ΔH and molar binding ratio of wtIL-5 (Table 2) are very similar to values measured by calorimetry with *Drosophila*-expressed hIL-5 (4). The steeper transition curve seen for wtIL-5 compared with DABC and GM1 reflects its 15-fold higher affinity for IL-5R. The thermodynamic basis for the reduced affinity of the monomeric IL-5 constructs is difficult to ascertain from the parameters in Table 2 due to experimental error. The error is larger for determination of ΔH for the monomeric constructs because of their weaker affinity combined with the low concentrations of reactants studied.

For all three IL-5 forms, the receptor is titrated out by addition of a single mol of IL-5 per mol of IL-5R. In the case of wtIL-5, this pertains to a single covalent dimer per receptor and in the cases of DABC and GM1 this pertains to a single monomer per receptor. Molar binding ratios were determined by nonlinear least squares analysis of the data in Fig. 6 and are given in Table 2. Deviations from theoretical 1.0 are likely due to the inherent error in defining reactant concentrations by absorbance at 280 nm. In any case, the close agreement in molar binding ratios for monomeric and dimeric forms of IL-5 argues strongly that the receptor binds the same number of mols of each.

DISCUSSION

In this study, we have demonstrated that two different isomers of IL-5, denoted DABC and GM1, fold into stable monomers and are functionally active. Their binding affinities for IL-5Rα are weaker than that of dimers, consistent with the hypothesis (25) that in wtIL-5 both four-helix bundles surfaces help stabilize receptor assembly, though asymmetrically. Nonetheless, the monomers form 1:1 complexes with receptor α subunit, similarly as wtIL-5. These data show that the minimum pharmacophore in hIL-5 is contained in a single four-helix bundle domain.

That the circular permutant DABC is as active as GM1 is consistent with the view that the packed four-helix bundle, and not connectivity between helices, is the key structural feature on which receptor binding epitopes are displayed in IL-5. The similar activities of DABC and GM1 in both IL-5Rα binding and signal transduction (Tables 1 and 2) suggest that the receptor-binding epitopes of both, including those in IL-5 loop sequences, are displayed in a similar way. Further, the data argue that N- and C-terminal residues *per se* are not critical to function. Nonetheless, DABC and GM1 both bind to IL-5Rα with a lower affinity than wtIL-5 (≈40-fold less). One explanation for the lower affinity is that the insertion of linkers induces slight perturbation of functional residues. However, DABC and GM1 have linkers in different regions and yet showed similar human receptor affinity. During this current study, we also have replaced the linker in GM1 with two other linkers (one without cysteine, one with a shorter linker) and still get the same receptor binding kinetics (data not presented). Taken together, our results suggest that receptor binding epitopes in hIL-5 are not very sensitive to variations in helix linking.

Since both hIL-5 and IL-5 of other species are dimeric and function through similar dual α/β_c receptors, it is tempting to

Table 2. Receptor binding properties of dimeric and monomeric forms of IL5 from titration calorimetry

IL-5 construct	Molar ratio (IL5/receptor)	K_d, nM	ΔG, kcal/mol	ΔH, kcal/mol	$-T\Delta S$ (kcal/mol)
wtIL5	0.72	14	−10.9 ± 0.6	−17.5 ± 0.6	6.6 ± 0.8
DABC	0.61	190	−9.3 ± 0.6	−17.7 ± 3.0	8.4 ± 3.1
GM1	0.60	220	−9.2 ± 0.6	−19.2 ± 3.0	10 ± 3.1

Error in K_d's values is about a factor 2-3. Conditions are as follows: 10 mM $NaPO_4$, and 150 mM NaCl (pH 7.4 at 30°C).

generalize that structural features important for hIL-5 are important for all IL-5s. Nonetheless, one observation made in the current study with human and mouse cell proliferation assays warns against carrying homology arguments too far. While the monomeric IL-5 isomers DABC and GM1 both exhibited a strong proliferative stimulation of human origin TF-1.28 cells, only GM1 stimulated a significant response with the murine-derived B13 cells, and this was some 20-fold less than that obtained with wild-type hIL-5. This differential argues that there are components in the human protein important for mouse receptor interaction and signal triggering that are retained in one monomeric isomer but not the other. It is not possible to deduce what structural element or elements may be at the root of this, but further mutation and isomerization of IL-5 structure may provide clues, as would direct mutagenesis of murine IL-5.

The current results lead inevitably to the often-asked question of why IL-5 is dimeric while the two other closely related members of its hematopoietic growth factor family, namely IL-3 and GM-CSF, are monomeric. Our data show functionality of two mono 5 isomers, the sufficiency of 1:1 stoichiometry for functional receptor recruitment and the monomer as the minimum pharmacophore for IL-5 action. So, what does the dimer structure provide? Based on the current results, there are at least three properties enhanced by dimerization: increased stability, increased receptor affinity, and increased cell proliferative response. That all three of these features make wtIL-5 a more potent growth factor than it could be as monomer is evident. Whether any one of these has been dominant in promoting survival of IL-5 as dimer is not possible to assert unambiguously as yet.

Beyond the current investigation, monomeric isomers promise to provide useful tools to investigate structure–function relationships in IL-5. Since monomer contains only half the sequence content of dimer, this engineered construction may provide a simplified structure for mutagenesis studies, in particular by epitope randomization of phage displayed protein. The monomer, again possibly coupled with phage libraries, may provide a useful tool to search for IL-5 isomers with improved receptor binding affinity, as has been shown previously with human growth hormone (31).

1. Kay, A. B. (1991) *Int. Arch. Allergy Appl. Immunol.* **94,** 189–193.
2. Sanderson, C. J. (1992) *Adv. Pharmacol.* **23,** 163–177.
3. Milburn, M. V., Hassell, A. M., Lambert, M. H., Jordan, S. R., Proudfoot, A. E. I., Graber, P. & Wells, T. N. C. (1993) *Nature (London)* **363,** 172–176.
4. Johanson, K., Appelbaum, E., Doyle, M., Hensley, P., Zhao, B., *et al.* (1995) *J. Biol. Chem.* **270,** 9459–9471.
5. Bennett, M. J., Schlunegger, M. P. & Eisenberg, D. (1995) *Protein Sci.* **4,** 2455–2468.
6. Feng, Y., Klein, B. K., Vu, L., Aykent, S. & McWherter, C. A. (1995) *Biochemistry* **34,** 6540–6551.
7. Diederichs, K., Boone, T. & Karplus, P. A. (1991) *Science* **254,** 1779–1782.
8. Tavernier, J., Devos, R., Cornelis, S., Tuypens, T., Van der Heyden, J., Fiers, W. & Plaetinck, G. (1991) *Cell* **66,** 1175–1184.
9. Lopez, A. F., Elliott, M. J., Woodcock, J. & Vadas, M. A. (1992) *Immunol. Today* **13,** 495–500.
10. Devos, R., Guisez, Y., Cornelius, S., Verhee, A., Van der Heyden, J., Manneberg, M., Lahm, H. W., Fiers, W., Tavernier, J. & Plaetinck, G. (1993) *J. Biol. Chem.* **268,** 6581–6587.
11. Dickason, R. R. & Huston, D. P. (1996) *Nature (London)* **379,** 652–655.
12. Dickason, R. R., English, J. D. & Huston, D. P. (1996) *J. Mol. Med.* **74,** 535–546.
13. Goldenberg, D. P. (1989) *Protein Eng.* **2,** 493–495.
14. Pan, T. & Uhlenbeck, O. C. (1993) *Gene* **125,** 111–114.
15. Yang, Y. R. & Schachman, H. K. (1993) *Proc. Natl. Acad. Sci. USA* **90,** 11980–11984.
16. Buchwalder, A., Szadkowski, H. & Kirschner, K. (1992) *Biochemistry* **31,** 1621–1630.
17. Zhang, T., Bertelsen, E. Benvegnu, D. & Alber T. (1993) *Biochemistry* **32,** 12311–12318.
18. Kreitman, R. J., Puri, R. K., McPhie, P. & Pastan I. (1995) *Cytokine* **7,** 311–318.
19. Li, J., Cook, R., Dede, K. & Chaiken, I. (1996) *J. Biol. Chem.* **271,** 1817–1820.
20. Morton, T., Li, J., Cook, R. & Chaiken, I. (1995) *Proc. Natl. Acad. Sci. USA* **92,** 10879–10883.
21. Summers, M. D. & Smith, G. E. (1987) *A Manual of Methods for Baculovirus Vectors and Insect Cell Culture Procedures* (Texas A&M Agricultural Exp. Station), 2nd Ed., Bull. No 1555.
22. Hensley, P. (1996) *Structure* **4,** 367–373.
23. Chan, W., Helms, L. R., Brooks, I., Lee, G., Ngola, S., McNulty, D., Maleef, B., Hensley, P. & Wetzel, R. (1996) *Folding Design* **1,** 77–89.
24. Laue, T. M., Shah, B. D., Ridgeway, T. M. & Pelletier, S. M. (1992) in *Analytical Ultracentrifugation in Biochemistry and Polymer Science*, eds. Harding, S. E., Rowe, A. J. & Horton, J. C (Royal Soc. of Chem., Cambridge, UK), pp. 90–125.
25. Li, J., Cook, R. & Chaiken, I. (1996) *J. Biol. Chem.* **271,** 31729–31734.
26. Morton, T., Bennett, D. B., Appelbaum, E. R., Cusimano, D., Johanson, K. O., Matico, R. E., Young, P. R., Doyle, M. L. & Chaiken, I. M. (1994) *J. Mol. Recognition* **7,** 47–55.
27. Pace, C. N., Vajdos, F., Fee, L., Grimsley, G. & Gray, T. (1995) *Protein Sci.* **4,** 2411–2423.
28. Wiseman, T., Williston, S., Brandts, J. F. & Lin, L.-N. (1989) *Anal. Biochem.* **179,** 131–137.
29. Eftink, M. R. (1995) *Methods Enzymol.* **259,** 487–512.
30. Ames, R. S., Tornetta, M. A., McMillan, L. J., Kaiser, K. F., Holmes, S. D., Appelbaum, E., Cusimano, D. M., Theisen, T. W., Gross, M. S., Jones, C. S., Silverman, C., Porter, T. G., Cook, R. M., Bennett, D. & Chaiken, I. M. (1995) *J. Immunol.* **154,** 6355–6364.
31. Lowman, H. B. & Wells, J. A. (1993) *J. Mol. Biol.* **234,** 564–578.